small NANO MICRO

Nanopores

The Passage of Homopolymeric RNA through Small Solid-State Nanopores

*Michiel van den Hout, Gary M. Skinner, Sven Klijnhout, Vincent Krudde, and Nynke H. Dekker**

Solid-state nanopores are widely acknowledged as tools with which to study local structure in biological molecules. Individual molecules are forced through a nanopore, causing a characteristic change in an ionic current that depends on the molecules' local diameter and charge distribution. Here, the translocation measurements of long (~5-30 kilobases) single-stranded poly(U) and poly(A) molecules through nanopores ranging from 1.5 to 8 nm in diameter are presented. Individual molecules are found to be able to cause multiple levels of conductance blockade upon traversing the pore. By analyzing these conductance blockades and their relative incidence as a function of nanopore diameter, it is concluded that the smallest conductance blockades likely correspond to molecules that translocate through the pore in predominantly head-to-tail fashion. The larger conductance blockades are likely caused by molecules that arrive at the nanopore entrance with many strands simultaneously. These measurements constitute the first demonstration that single-stranded RNA can be captured in solid-state nanopores that are smaller than the diameter of double-stranded RNA. These results further the understanding of the conductance blockades caused by nucleic acids in solid-state nanopores, relevant for future applications, such as the direct determination of RNA secondary structure.

1. Introduction

The rapid detection of biological molecules' local structure can be very useful for the study of molecular conformations or local binding. A technique that can probe molecular structure on the nanometer-scale in liquid is that of solid-state nanopores (for a recent review, see Reference [1]). In this technique, individual molecules are mechanically or electrically forced through the nanopore, causing a temporary blockade of an ionic current passing through the pore. The duration of this blockade can report on the molecules' length or degree of folding,[2] while its magnitude reports on the molecules' local size and charge distribution inside the nanopore.[3–6] Using this approach, it is possible to detect the presence of double-stranded[7] and single-stranded nucleic acids,[8,9] and to distinguish single-stranded from double-stranded nucleic acids within the same sample.[10] Similarly, solid-state nanopores have been utilized to detect individual proteins[11] or to study the binding of proteins or small molecules to DNA.[12–15] The smaller the dimensions of such nanopores, the more effectively they can be expected to report on local variations in molecular structure. For instance, the effect of the applied voltage on the translocation of single- and double-stranded DNA in nanopores of diameters ~2 nm and smaller has been studied both experimentally[16] and via simulations,[17] reporting on stretched conformations of duplex DNA. Additionally, the unzipping of DNA hairpin structures in pores of these dimensions has been investigated.[18] Such local structure detection could be particularly useful for the study of RNA molecules, as the structures of many RNA molecules remain unknown.[19] For example, RNA molecules

Dr. M. van den Hout, Dr. G. M. Skinner, S. Klijnhout, V. Krudde, Prof. N. H. Dekker
Department of Bionanoscience
Kavli Institute of Nanoscience
Delft University of Technology
Lorentzweg 1, 2628 CJ Delft, The Netherlands
E-mail: N.H.Dekker@tudelft.nl

DOI: 10.1002/smll.201100265

could potentially be (mechanically[6,20–22]) forced through nanopores with a diameter smaller than that of double-stranded RNA, allowing their secondary structure elements to be unfolded. In contrast to previously employed single-molecule methods such as optical tweezers,[23,24] this approach would permit unfolding in a sequential manner.[25,26]

With this goal in mind, we studied how RNA molecules traverse nanopores with diameters down to 1.5 nm in diameter, well below the diameter required for the unfolding of any secondary structure. As any detection of folding rests on the ability to differentiate folded from unfolded structures, it is essential to first explore how unfolded structures interact with nanopores in this size limit. We have therefore focused our study on largely unstructured[27–31] single-stranded homopolymeric poly(U) and poly(A) RNA molecules, showing that even these simple molecules can cause two readily distinguishable levels of conductance blockade through their interaction with small nanopores, and we study this phenomenon as a function of the nanopore diameter (ranging from 1.5 to 8 nm). We find that the population associated with the largest conductance blockades ($\Delta G \approx 3$ nS or higher) occurs most frequently in the smallest nanopores, but occurs only rarely in the largest nanopores. At the same time, the magnitude of the largest conductance blockade typically increases in magnitude as the nanopore size is increased. In contrast, the population associated with smaller conductance blockades (~1–2 nS) is most frequently present in large nanopores while it is absent from the smallest nanopores. For this population, the magnitude of the conductance blockade is found to be largely independent of the nanopore size (with the exception of nanopores with diameters below 2.5 nm).

Based on these observations, we deduce that the population associated with the smallest blockades likely corresponds to RNA molecules that translocate through the nanopore in predominantly head-to-tail fashion (in which the molecule traverses the nanopore as a single string that is reeled through the nanopore): the magnitude of the conductance blockade of such translocations should be approximately independent of nanopore diameter. Furthermore, such translocations would be increasingly unlikely in the smallest nanopores, in accordance with our observations. In contrast, the population associated with the largest blockades is likely to correspond to instances in which many RNA strands (of a single molecule) simultaneously converge on the nanopore entrance. As the voltages we apply are typically quite high (300–500 mV), some of these molecules may still traverse the nanopore in folded fashion, while leading to a significantly higher (and less well-defined) blockade level than the head-to-tail translocations observed in the larger nanopores.

Interestingly, we also show that in some cases the population associated with small conductance blockades (~1–2 nS) displays substructure, allowing us to distinguish subpopulations whose conductance blockades are shown to be integer multiples of each other. This is reminiscent of results reported previously using double-stranded DNA molecules (dsDNA) in nanopores of about 10 nm in diameter.[7,32] There, the existence of subpopulations was attributed to partially folded DNA molecules simultaneously occupying the pore with two or even more (duplex) strands during translocation, with each DNA strand contributing a quantized amount to the conductance blockade. Those measurements indicated that, for DNA, pure head-to-tail translocations are properly identified with the subpopulation demonstrating the lowest conductance blockade. Our analogous observation of subpopulations with conductance blockades that are integer multiples of each other for homopolymeric RNA suggests that a similar identification can be made: the subpopulation with the lowest conductance blockade corresponds to pure head-to-tail translocations. In addition, as the conductance blockades of this ensemble of subpopulations remain very readily distinguishable from the population characterized by large conductance blockades (~3 nS and higher), this further suggests that the latter population represents a different type of interaction of the RNA molecules with the nanopore (e.g., via a much higher and less well-defined number of strands).

These combined results contribute to the further understanding of the conductance blockade caused by biological molecules in solid-state nanopores, and provide guidelines for experiments designed to probe the unfolding of RNA secondary structure through nanopores.

2. Results and Discussion

To investigate the translocation of RNA through molecular-sized nanopores, we employ a setup as shown in **Figure 1**a. A nanopore separates two chambers (*cis* and *trans*) containing an ionic solution. Electrodes are inserted into both chambers to apply a positive bias voltage (towards the *trans* chamber), causing an ionic current to flow through the nanopore. In addition, the electrical field will force negatively charged RNA molecules (introduced into the *cis* chamber) through the nanopore, causing a temporary blockade (ΔI) of the ionic current (Figure 1b).

Before discussing the results in the smallest nanopores, we will first describe a typical experiment using a relatively large nanopore of 8 nm in diameter, an example of which is shown in Figure 1c. Here, we have introduced a sample of long, polydisperse (5–30 kb) homopolymeric poly(U) molecules into the *cis* chamber, and we start the experiment by applying a negative potential of –300 mV towards the *trans* chamber. At this negative bias voltage, the molecules do not translocate through the nanopore (as they are negatively charged), which is reflected in the constant nanopore conductance. At time $t \approx 3$ s we reverse the voltage to a positive bias and find that the nanopore conductance is now frequently interrupted by small (downward) spikes, presumably corresponding to molecules that temporarily block the current while passing through the nanopore. To verify whether molecules indeed translocate through the nanopore, after a few seconds we once again apply a negative bias (Figure 1c, $t \approx 7$ s; note that the small transient observed in the conductance is a consequence of the capacitive coupling of the nanopore membrane). While previously no spikes were observed at this bias voltage, we now see the appearance of small spikes that have a magnitude similar to that of the spikes observed at positive bias. However, the spikes are much less frequent and completely disappear within several seconds. These observations

NANO MICRO small

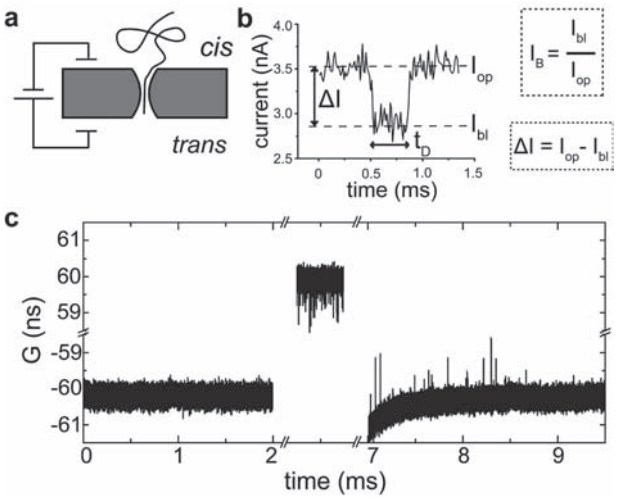

Figure 1. Experimental setup and example trace of translocating poly(U) molecules. a) Schematic of the setup employed. A nanopore immersed in electrolyte separates two compartments (*cis* and *trans*). After introduction of RNA on the *cis* side, an external bias voltage can thread RNA molecules through the nanopore, causing the ionic current to be partially blocked. b) Sample trace of the current blockade caused by an RNA molecule in a 2.5 nm diameter pore at 300 mV bias voltage. For each translocation event we determine the average blockade $\Delta I = I_{op} - I_{bl}$ as the current in the open state (I_{op}) minus the current in the blocked state (I_{bl}), the dwell time t_D as the total duration of the event, and the relative current blockade $I_B = I_{bl}/I_{op} = 1 - \Delta I/I_{op}$. c) Example demonstrating the actual translocation of RNA molecules through an 8 nm diameter nanopore. Prior to the experiment, RNA molecules are introduced on the *cis* side. The initial application of a negative bias voltage (at $t = 0$ s) does not induce any downward spikes in the nanopore conductance, as the *trans* chamber contains no RNA molecules. However, application of a positive voltage (after $t = 2$ s) induces many downward spikes in the conductance, indicating the translocation of RNA molecules through the nanopore. Indeed, after again reversing the voltage ($t = 7$ s) some spikes also appear at negative bias voltage, indicating the *trans* chamber now contains RNA molecules that translocate towards the *cis* chamber. After maintaining this polarity for a while, the continued appearance of spikes ceases, as the local concentration on the *trans* side near the nanopore rapidly decreases due to diffusion of the molecules away from the nanopore.

are exactly as expected provided that a reasonable fraction of the spikes at positive bias voltage corresponds to translocating molecules; such translocated molecules can reverse their direction at negative bias voltage and once again contribute to spikes in the conductance. We note that the rate at which spikes occur at negative bias is much reduced, which is expected since diffusion of the translocated molecules in the *trans* chamber will rapidly decrease the local concentration in the vicinity of the nanopore. Thus, this experiment demonstrates the successful translocation of RNA molecules through our solid-state nanopores.[10,33]

We now investigate the magnitude and duration of the observed spikes in the conductance. In **Figure 2**a we show 1D histograms of the conductance blockade ΔG and dwell time t_D (right and top, respectively) for conductance blockade events recorded with poly(U) molecules in an 8 nm diameter pore at +300 mV bias voltage, as well as a 2D histogram of the conductance blockade (expressed both as ΔG (right axis) and as I_B (left axis); for the definition of I_B, see Figure 1b and the Experimental Section) versus t_D. From the 2D histogram, we observe that the events are clearly distributed into a single population with roughly similar dwell times and conductance blockades. This is also reflected in the 1D conductance histogram, which shows a single peak at nonzero ΔG (the additional peak at $\Delta G = 0$ nS simply reflects the open pore current surrounding events; see Experimental Section). This peak, reflecting the distribution of the average blockade level of events that are distinguishable above the baseline noise (Experimental Section), has a mean value of $\Delta G = 0.7 \pm 0.3$ nS, as determined by fitting to a Gaussian distribution. This value is similar to the value $\Delta G = 0.65 \pm 0.05$ nS reported earlier for the translocation of such molecules in similarly sized nanopores[10] at this bias voltage. From the 1D dwell time histogram of the events, we can see that most events are very short (<1 ms), with the majority having a duration of approximately 200 μs.

To investigate the behavior of RNA in smaller nanopores, we show in Figure 2b a similar 2D histogram of the events for poly(U) molecules interacting with a 2.5 nm diameter nanopore at +300 mV bias voltage. The scale of the conductance blockade ΔG is identical to that of Figure 2a; however, we have employed a different scale for the I_B axis, a direct consequence of the much reduced open pore current through the smaller nanopore. In a nanopore of this size, we first observe that the events are no longer distributed into a single population that has approximately uniform values of the dwell time and conductance blockade. Rather, two populations are visible, with clearly different I_B values and much extended dwell times. To make this more precise, we refer to the 1D conductance histogram (Figure 2b, right), which now exhibits *two* peaks in addition to the baseline peak (which, as above, merely reflects the open pore conductance): a population with a lower conductance blockade and a population with a higher conductance blockade. Interestingly, both we and others[34,35] have previously reported a similar separation into distinguishable event populations for DNA molecules interacting with small nanopores in this size range (diameters ranging from ~2 to 7 nm). Following our previously reported definitions,[34] we denote the first group ***H***-events, and the second group **L**-events, the nomenclature reflecting high and low values of I_B, respectively (Experimental Section). By fitting to Gaussian distributions as above, we determine that the peak in the 1D conductance histogram corresponding to the ***H***-events is closest in both ΔG value ($\Delta G = 1.5 \pm 0.5$ nS) and width to the peak in Figure 2a for the 8 nm nanopore, suggesting that the ***H***-events in the 2.5 nm nanopore may correspond to the same type of events as observed in the larger pore, established above to correspond (at least in part) to actual translocations (Figure 1c).

To understand why we observe a population with a large conductance blockade (the ***L***-population) in the small 2.5 nm nanopore but not in the larger 8 nm nanopore, we have investigated how the ***H***- and ***L***-populations evolve as the nanopore diameter is decreased from 8 to 1.5 nm. For each nanopore diameter, we have determined the percentage of events in the ***H***- and ***L***-population (see Experimental Section

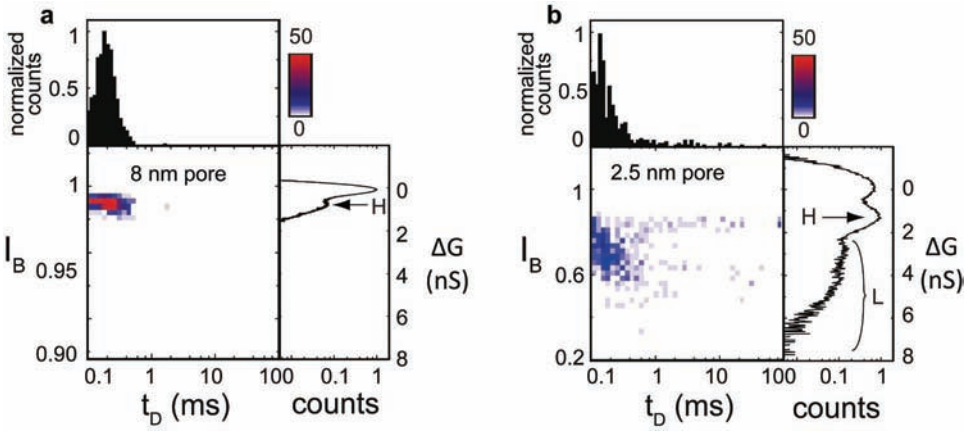

Figure 2. 2D histograms of I_B versus t_D for poly(U) in two different nanopores along with their 1D projections. a) Histograms for poly(U) events acquired in an 8 nm pore (resistance, $R = 17 \pm 0.7$ MΩ, and number, $N = 1071$ events). The 2D histogram of the event frequency as a function of current blockade I_B versus t_D. Events appear to be distributed into a single population. The 1D histogram on the right is employed in determining the mean ΔG for different populations: here, we histogram the number of datapoints at a given ΔG (or I_B) over all events, whereby the nontrivial, lowermost peak is identified as ***H*** (the uppermost peak results from the trivial contribution of the open pore current that surrounds events, see Experimental Section). Note that the counts in this histogram are normalized by the counts in the maximally occupied bin. The 1D histogram on the top is a direct projection of the 2D histogram showing the dwell time distribution of the individual events. b) Similar histograms for poly(U) events acquired in a 2.5 nm pore ($R = 116 \pm 3$ MΩ, $N = 420$ events). Note the different scale for I_B in the two panels. In this nanopore we observe two groups of events: one with small conductance blockade ($\Delta G = 1.5 \pm 0.5$ nS) and small variation in blockade, indicated as ***H*** and one with a larger blockade and larger variation ($\Delta G = 4.2 \pm 2$ nS), indicated as ***L***. As in (a), the counts in the 1D conductance histogram are normalized by the counts in the maximally occupied bin. The dwell time distribution of the events in the 2.5 nm pore is also significantly broader than in the 8 nm pore.

for details). The result is shown in **Figure 3**, where we plot the percentage of ***L***-events versus nanopore diameter for poly(U) molecules at 300 mV. Since the percentage of ***L***- and ***H***-events are roughly anticorrelated (%***H*** ≈ 100% –%***L***, see Experimental Section), the plot indirectly also contains information on the ***H***-events. The solid line is shown as a guide to the eye. It is clear that the percentage of ***L***-events gradually increases, from 0% to about 75–100%, as the nanopore diameter is decreased from 8 nm down to 1.5 nm. It thus appears that the ***L***-population is only present to a significant extent in nanopores with diameters beneath ~4 nm. Concurrently, the ***H***-events gradually disappear with decreasing nanopore size. Since we have already shown in Figure 1c that the ***H***-population in the larger nanopores corresponds (at least in part) to actual translocations, it comes as no surprise that this population would gradually disappear when the nanopore diameter is decreased: the smaller the nanopore, the less likely the molecule will be able to translocate.

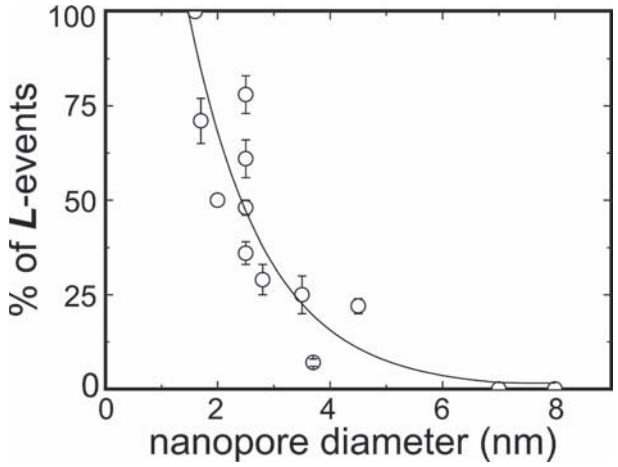

Figure 3. Percentage of ***L***-events for nanopores of ranging from 1.5 to 8 nm in diameter. ***L***-events only appear in nanopores smaller than 5 nm in diameter and increase dramatically as the nanopore size is reduced below 2.5 nm. Since events are always either ***H***- or ***L***-events, the graph also contains information on the ***H***-events (%***H*** = 100% –%***L***, see Experimental Section). The ***H***-events thus gradually disappear with decreasing nanopore diameter. The solid line is a guide to the eye. The size of the error bar equals one half the number of multilevel events (in which a single event reaches multiple levels). See Experimental Section.

To further clarify the origin of the ***L***-population, we have compared the magnitude of the conductance blockade ΔG of both the ***H***- and ***L***-populations over the same range of pore sizes as above (**Figure 4**a; ***H***-population shown with filled circles and ***L***-population shown with open circles). Recall from our discussion of Figure 2a,b that the average conductance blockade of the ***L***-population in the 2.5 nm pore exceeded that of the ***H***-population: $\Delta G = 4 \pm 2$ nS compared to $\Delta G = 1.5 \pm 0.5$ nS, respectively, and that the average conductance blockade ΔG of the ***H***-population was very similar in 2.5 and 8 nm nanopores. Both of these trends are confirmed as the nanopore diameter is varied: first, the conductance blockade of the ***L***-events is consistently larger than that of the ***H***-events, and is found to increase with increasing nanopore diameter (until the entire ***L***-population vanishes for the largest nanopores); second, to a first approximation the conductance blockade ΔG of the ***H***-events appears to be independent of nanopore diameter (a slight decrease in

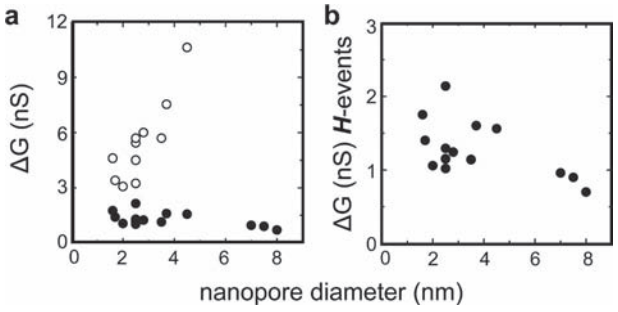

Figure 4. Dependence of the conductance blockade Δ*G* on nanopore diameter for poly(U) molecules ranging between 5–30 kb in length. a) Conductance blockade of the ***H***- (closed circles) and ***L***-events (open circles) versus nanopore diameter. The blockade of the ***L***-events gradually increases as the nanopore size is increased (until the ***L***-events completely disappear in nanopores larger than 5 nm in diameter, see Figure 3). In contrast, the conductance blockade of the ***H***-events decreases somewhat with increasing nanopore diameter, as can be seen in panel (b), which displays a zoom of only the ***H***-events.

the Δ*G* for the ***H***-events is in fact observed with increasing nanopore diameter (see the zoomed portion of Figure 4b), but the variation in Δ*G* is much less pronounced than in the case of the ***L***-events). Note that in principle a detailed investigation of the dwell times versus pore diameter might illuminate further differences between ***H***- and ***L***-populations, but we find that relatively little additional information can be unearthed from such an investigation for this case of homopolymeric RNA molecules with a wide distribution of lengths (Figure S1 in the Supporting Information). Interestingly, however, these trends are very similar to those observed for long duplex DNA translocated through solid-state nanopores of varying sizes[34] and, in the case of large blobs of single-stranded DNA, to the observations of an increased conductance blockade Δ*G* as a function of the applied voltage.[9]

We now discuss possible explanations for these observations, starting first with the ***H***-events. Assuming that these events indeed correspond to predominantly head-to-tail translocations, one might expect the conductance blockade Δ*G* to be independent of the nanopore diameter: after all, the number of ions blocked during the translocation should only depend on the volume and charge distribution of the molecule inside the nanopore. However, there are at least two phenomena that can cause the measured value of Δ*G* to deviate from its expected behavior. First, for nanopore sizes close to the diameter of the translocating molecule the nanopore walls will start to affect the cloud of counterions shielding the molecule and thus change the magnitude of Δ*G*. This effect has also been observed for DNA and led to an increase in Δ*G* in nanopores below 3.2 nm in diameter.[6,34] With an estimated diameter of poly(U) molecule of about 1 to 1.5 nm[10] (the bases can randomly orient themselves in all directions around the phosphate backbone), we expect this effect may come into play when the nanopore diameters are reduced to 2–2.5 nm. Second, in large nanopores the dwell times start to approach the detection limit (see for example Figure 2a), which often leads to an underestimation of Δ*G* in larger nanopores. These two effects can explain the overall trend observed for the conductance blockade of the ***H***-events.

We now propose a scenario that takes into account the Δ*G* of the ***L***-events and its gradual increase with increasing nanopore diameter (Figure 4a). To start, the observation that the blockade of the ***L***-events is overall much larger than that of the ***H***-events indicates that these events are likely caused by a different type of interaction with the nanopore. A likely explanation for this higher blockade is that the molecule enters the nanopore entrance with many strands simultaneously (e.g., as a dense blob), yielding a much higher blockade than would a single strand alone.[9,34] This could be facilitated by the high flexibility of single-stranded RNA molecules, whose persistence length (approximately 1 nm for poly(U)[30]) is small compared to the entry region of the nanopore. The fact that the entrance of our nanopores is typically significantly wider than the smallest constriction in the pore,[36,37] further renders it more likely that a molecule could enter the nanopore's aperture with multiple strands simultaneously. If correct, one would then expect the conductance blockade of ***L***-events caused by such molecules to fluctuate heavily, as a result of the varying number of strands inside the nanopore. Indeed, we already observed that the spread in Δ*G* of the ***L***-population is much larger than that of the ***H***-population (Figure 2a), an effect that generally holds true across all measurements. Even within a single event, the conductance blockade for an ***L***-event typically shows much more variation than that of an ***H***-event. We note that the observed trend of Δ*G* of the ***L***-events with varying nanopore diameter can similarly be accounted for by this scenario: a larger pore would permit more strands to fit into the nanopore simultaneously, thus leading to an average higher Δ*G* for these nanopores. Finally, the proposed mechanism can explain the observation that ***L***-events primarily occur in the smallest nanopores: for smaller nanopores, it is more likely that a molecule captured in the vicinity of the nanopore entrance would (temporarily) interact with the nanopore surfaces. During this time, it is likely that other strands in the vicinity of the nanopore become pulled into the nanopore entrance. This would be less likely in larger nanopores since the likelihood of adhering in the entrance region is reduced, while furthermore the force on the molecule is lower in larger nanopores.[6] Entropic forces from the rest of the coil (outside the influence of the electrical field) can then more easily prevent multiple strands from being pulled simultaneously into the nanopore, thus favouring the head-to-tail translocations that we typically observe in larger nanopores.

The proposed scenario underlying the observation of ***L***-events raises the question whether one can observe different sublevels in this population, each reflecting the behavior of molecules with a precise number of strands in the nanopore. Indeed, individual ***L***-events do often show substructure, but unfortunately the significant variation between the different events often washes out any such substructure, and no overall trend could be distinguished. For the ***H***-events, however, we have occasionally observed very clear substructure in nanopores with diameters between 3 and 5 nm. An

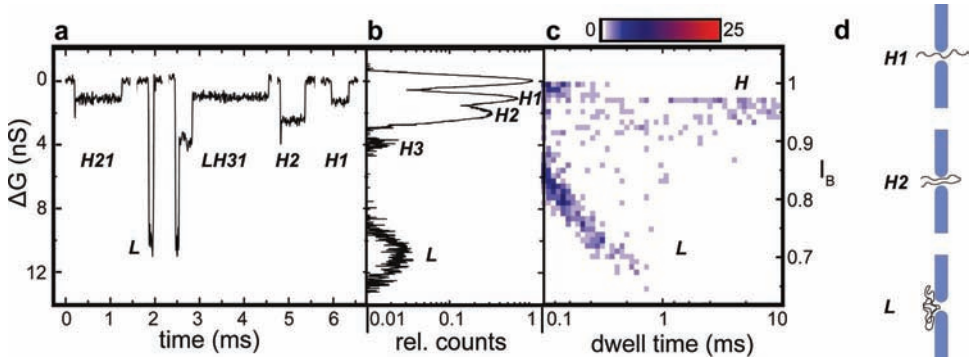

Figure 5. Example of substructure in ***H***-events for poly(A) molecules in a 5 ± 2 nm nanopore at 300 mV. a) Example traces of individual conductance blockade events. Events can have single or multiple blockade levels and are labelled according to the different conductance blockade levels they comprise (see Experimental Section and panel (b) for level assignments). Thus, an ***H21*** event first experiences the conductance blockade level associated with an ***H2*** event and subsequently the conductance blockade level associated with an ***H1*** event. b) The 1D conductance histogram (normalized as described in the caption to Figure 2a) shows three blockade levels with small Δ*G*, labelled ***H1***, ***H2,*** and ***H3***. The ***H2*** and ***H3*** levels are located at nearly integer multiples of the Δ*G* value of the H1 level, indicating that these correspond to integer numbers of strands traversing the nanopore simultaneously. The ***L***-level has a significantly higher Δ*G* value and has a wider spread. c) 2D histogram of the events recorded in this nanopore. Note that the I_B values of the ***L***-group vary much more than in the 1D conductance histogram in (b), because most of these events are multilevel (e.g., ***LH2***), leading to a lower average Δ*G* value (and a correspondingly higher I_B). d) Pictorial representation of the event types ***H1***, ***H2***, and ***L***.

example of this is shown in **Figure 5**, where we used poly(A) molecules in a 5 ± 2 nm diameter nanopore at 300 mV. From the 1D histogram (Figure 5b) we can see the peak corresponding to the ***H***-events (Δ*G* = 1.1 ± 0.4 nS, labeled ***H1***, where the error reflects the width of a Gaussian fit to the peak) directly below the peak corresponding to the open pore current. However, two additional peaks can be observed at Δ*G* = 2.0 ± 0.7 nS (labeled ***H2***) and Δ*G* = 4.0 ± 1.7 nS (labeled ***H3***). Within error, these values are, interestingly, integer multiples of the ***H1***-peak, which would be expected if the first ***H***-peak corresponds to a single strand of poly(A) inside the nanopore, the second to two (Figure 5d), and the third to three strands. These results suggest that, in those cases, the conductance alone can report on the local substructure along a single RNA molecule, in a manner analogous to previous observations on the behavior of duplex DNA in larger pores.[32] We point out that even the third (***H3***) peak can still clearly be distinguished from the peak of the ***L***-events (with Δ*G* = 10.8 ± 3.1 nS), suggesting that the ***L***-events indeed correspond to a different mechanism in which even more strands in a less defined conformation obstruct the nanopore. Following the scenario sketched above, we surmise that the ***L***-events are different in that the nanopore entrance becomes obstructed with a multitude of RNA strands during the translocation of the RNA, whereas in the case of ***H1***-, ***H2***-, and ***H3***-events, the nanopore entrance remains open (Figure 5d).

3. Conclusion

We have presented conductance blockade events of homopolymeric poly(U) and poly(A) RNA molecules passing through nanopores ranging from 1.5 to 8 nm in diameter. As these molecules interact with the nanopore, we can distinguish different levels of conductance blockade. By investigating the magnitude and incidence of these different levels for different pore sizes, we surmise that the smallest blockade level (***H***-events) corresponds primarily to head-to-tail translocations, whereas the largest blockades (***L***-events) are caused by molecules that obstruct the entrance of the nanopore with many strands simultaneously. Furthermore, we show that in certain cases, the ***H***-events can reveal substructure corresponding to integer multiples of strands translocating the nanopore in a pure head-to-tail fashion. These results contribute to the general understanding of the conductance blockade caused by biological molecules in solid-state nanopores, which is required for future applications such as genomic screening or local structure determination along single molecules. Furthermore, we have shown for the first time that single-stranded RNA can translocate through solid-state nanopores with a diameter small enough to allow for the potential unfolding of double-stranded RNA. Simultaneously we have demonstrated that interpretation of the conductance blockade must take into account the possible presence of multiple strands in the pore's vicinity. Therefore we provide important guidelines for experiments designed to determine RNA secondary structure using solid-state nanopores.

4. Experimental Section

Nanopore Fabrication: Fabrication of our nanopores is described in detail elsewhere.[38] In brief, we use a highly focused transmission electron microscope (TEM) beam to drill a nanopore into a 20 nm thick SiN membrane. To optimize the stability of our nanopores,[36] we have typically used a TEM beam size (full width at half maximum) approximately equal to the diameter of the nanopore, giving rise to an hour-glass-shaped nanopore profile. Nevertheless, in some cases the nanopore conductance was found to increase during the experiments, which we have previously shown to be caused by a physical increase in diameter of the

NANO MICRO small

nanopore.[36] For the measurements presented here, only results in which the nanopore conductance did not change more than 25% during the experiment (corresponding to a change in diameter of approximately 10–15%) were included.

Experimental Details: Following fabrication, nanopores were stored in a solution containing 50% ethanol (EtOH) and 50% ddH_2O (deionized water that was UV-treated and filtered through 20 nm pores). Prior to use, the nanopores were rinsed with ddH_2O, acetone, and EtOH, blown dry, and subjected to O_2 plasma for 20 s. Afterwards the samples were placed in a custom-made flow cell and flushed on both sides with ddH_2O, followed by 200 μL of measurement buffer (1 M KCl, 10 mM Tris-HCl (pH = 8.0) and 1 mM ethylenediaminetetraacetic acid (EDTA)). AgCl-coated electrodes were inserted on both sides of the nanopore, and the conductance was recorded (using an Axopatch 200B) for several seconds to establish that no events were observed and the nanopore conductance was stable. Next, measurement buffer containing poly(U) or poly(A) molecules was introduced on the *cis* side (Figure 1a), and a bias voltage of 300 mV was applied over the nanopore. Actual translocation of the molecules was experimentally verified by briefly recording translocations at positive bias voltage, and quickly reversing the bias voltage to observe translocations in the opposite direction (Figure 1c). These would typically occur only for several seconds, as most of the molecules on the *trans* side would already have diffused away from the nanopore. For the smallest nanopores such verification was not possible as the event rate is too small (higher concentrations to overcome this problem led to very fast clogging of the nanopores). The voltage and current were sampled at 90–200 kHz bandwidth. For every nanopore, several hundred to thousands of conductance blockade events (***N***) were collected at 300 mV bias voltage.

Molecule Synthesis: Poly(U) and poly(A) molecules were synthesized using the enzyme polynucleotide phosphorylase (PNPase, Sigma-Aldrich, USA). 4 μg of PNPase was incubated in 100 mM Tris-HCl buffer (pH = 9), supplemented with 5 mM $MgCl_2$, 0.4 mM EDTA, 0.04% w/v bovine serum albumin (BSA), and either 20 mM uridine diphosphate (UDP) (for poly(U)) or 20 mM adenosine diposphate (ADP) (for poly(A)). The reaction mixture was incubated at 37 °C for 15 min, subsequently purified and concentrated with RNeasy MiniElute Cleanup kit (Qiagen, USA) into a final volume of 30 μL of 1× TE (10 mM Tris-HCl (pH = 8.0), 1 mM EDTA), and finally stored at −20 °C until use. This template-independent synthesis reaction yields a polydisperse sample of long RNA molecules: using gel electrophoresis, we estimate the molecules to have lengths ranging from 5 kb to approximately 30 kb. Synthesis of reproducibly uniform length distributions using PNPase was found to be more reliable for poly(U) than for poly(A), as the latter shows an enhanced sensitivity to the initial ADP concentration: a decrease in the initial ADP concentration from 20 to 10 μM results in an approximately fivefold decrease in the average length of the final poly(A) product. For the translocation experiments, the molecules were diluted into a solution of 1 M KCl, 1× TE (pH = 8.0) to a final concentration of approximately 1–10 ng/μL.

Data Analysis: Traces containing conductance blockade events were low-pass filtered at 35 kHz and analyzed as described previously.[10] The typical requirement for the detection of an event was such that a minimum of 9 consecutive data points (corresponding to a minimum dwell time of 45–100 μs) must deviate from the average current by more than 4.5 times the standard deviation of the current (where the latter is determined in the absence of events). This criterion ensures that it is extremely unlikely that random fluctuations of the current will contribute false positives to the detected events. Each event was assigned a dwell time t_D and average conductance blockade expressed either as ΔG ($= \Delta I/V$) or I_B ($= I_{bl}/I_{op} = 1 - \Delta I/I_{op}$; Figure 1b), irrespective of whether an event was single-level or multilevel (see below).

To categorize the assignment of individual events into "types" such as ***H*** or ***L*** (Figure 2), we first determined the average conductance blockade for each of the two levels, ***H*** and ***L***, from Gaussian fits to the 1D conductance histogram comprised of all the events (Figure 2b, right). Occasionally, an additional peak was observed very close to the open pore current peak, which in the case of experiments on DNA in small nanopores we have previously assigned as the ***0***-level.[34] However, in the experiments on RNA presented here, this peak always corresponded to fewer than 2% of all events, and was therefore not taken into account. The midpoint of the average conductance blockade of the ***H***-events and that of the ***L***-events was then employed as a cutoff value in type attribution for individual events.

More precisely, each individual event was scanned point-by-point, and when the number of consecutive points in an event that fell between 4.5σ above the baseline current and the cutoff value exceeded a critical value (typically ~7), an ***H***-level was assigned; similarly, when the number of consecutive points in an event that fell above the cutoff value exceeded a critical value (typically ~7), an ***L***-level was assigned. Note that according to this algorithm, a single event that reached different blockade levels consecutively, would be classified as ***LH*** or ***HL*** or more complex versions (see Figure 5a). For multilevel attribution, the same minimum number of consecutive points was required for the event to be named accordingly. For example, an ***LH*** event must have minimally 7 consecutive points that are closest to the ***L***-level, followed by minimally 7 consecutive points that are closest to the ***H***-level. We note in particular that multilevel events are taken into account in the computation of the percentage of ***L***-events by adding one half of the percentage of multilevel events to the percentage of ***L***-events. This same number also determines the size of the error bar in the percentage of ***L***-events (Figure 3).

Finally, in some nanopores multiple levels of ***H***-events were observed, corresponding to the simultaneous blockage of the nanopore with two or more individual strands. The magnitude of the conductance blockades of these levels were typically integer multiples of the smallest ***H***-level, resulting in the naming, ***H1***, ***H2***, etc. (Figure 5).

Supporting Information

Supporting Information is available from the Wiley Online Library or from the author.

Acknowledgements

We thank X. Janssen, A. Hall, S. Kowalczyk, and M.-Y. Wu for help with nanopore fabrication, and S. Hage and S. Donkers for help

with RNA synthesis. Financial support is acknowledged from the Netherlands Organisation for Scientific Research (NWO), the Dutch Foundation for Research on Matter (FOM), and the European Science Foundation.

[1] C. Dekker, *Nat. Nanotechnol.* **2007**, *2*, 209.
[2] S. Kotsev, A. B. Kolomeisky, *J. Chem. Phys.* **2007**, *127*, 185103.
[3] S. Ghosal, *Phys. Rev. Lett.* **2007**, *98*, 238104.
[4] U. F. Keyser, S. van Dorp, S. G. Lemay, *Chem. Soc. Rev.* **2010**, *39*, 939.
[5] R. M. Smeets, U. F. Keyser, D. Krapf, M. Y. Wu, N. H. Dekker, C. Dekker, *Nano Lett.* **2006**, *6*, 89.
[6] S. van Dorp, U. F. Keyser, N. H. Dekker, C. Dekker, S. G. Lemay, *Nat. Phys.* **2009**, *5*, 347.
[7] J. Li, M. Gershow, D. Stein, E. Brandin, J. A. Golovchenko, *Nat. Mater.* **2003**, *2*, 611.
[8] D. Fologea, M. Gershow, B. Ledden, D. S. McNabb, J. A. Golovchenko, J. Li, *Nano Lett.* **2005**, *5*, 1905.
[9] S. W. Kowalczyk, M. W. Tuijtel, S. P. Donkers, C. Dekker, *Nano Lett.* **2010**, *10*, 1414.
[10] G. M. Skinner, M. Van Den Hout, O. Broekmans, C. Dekker, N. H. Dekker, *Nano Lett.* **2009**, *9*, 2953.
[11] D. Talaga, J. Li, *J. Am. Chem. Soc.* **2009**, *131*, 9287.
[12] R. M. Smeets, S. W. Kowalczyk, A. R. Hall, N. H. Dekker, C. Dekker, *Nano Lett.* **2009**, *9*, 3089.
[13] B. Hornblower, A. Coombs, R. D. Whitaker, A. Kolomeisky, S. J. Picone, A. Meller, M. Akeson, *Nat. Methods.* **2007**, *4*, 315.
[14] S. W. Kowalczyk, A. R. Hall, C. Dekker, *Nano Lett.* **2010**, *10*, 324.
[15] M. Wanunu, J. Sutin, A. Meller, *Nano Lett.* **2009**, *9*, 3498.
[16] U. Mirsaidov, J. Comer, V. Dimitrov, A. Aksimentiev, G. Timp, *Nanotechnology.* **2010**, *21*, 395501.
[17] J. Comer, V. Dimitrov, Q. Zhao, G. Timp, A. Aksimentiev, *Biophys. J.* **2009**, *96*, 593.
[18] B. McNally, M. Wanunu, A. Meller, *Nano Lett.* **2008**, *8*, 3418.
[19] K. E. Deigan, T. W. Li, D. H. Mathews, K. M. Weeks, *Proc. Natl. Acad. Sci. USA.* **2009**, *106*, 97.
[20] U. F. Keyser, Van Der Does, J. C. Dekker, N. H. Dekker, *Rev. Sci. Instrum.* **2006**, *77*, 105105.
[21] U. F. Keyser, B. N. Koeleman, S. van Dorp, D. Krapf, R. M. M. Smeets, S. G. Lemay, N. H. Dekker, C. Dekker, *Nano Lett.* **2006**, *2*, 473.
[22] M. van den Hout, I. D. Vilfan, S. Hage, N. H. Dekker, *Nano Lett.* **2010**, *10*, 701.
[23] J. Liphardt, B. Onoa, S. B. Smith, I. J. Tinoco, C. Bustamante, *Science.* **2001**, *292*, 733.
[24] B. Onoa, S. Dumont, J. Liphardt, S. B. Smith, I. Tinoco, Jr., C. Bustamante, *Science.* **2003**, *299*, 1892.
[25] U. Gerland, R. Bundschuh, T. Hwa, *Phys. Biol.* **2004**, *1*, 19.
[26] H. Vocks, D. Panja, G. T. Barkema, *J. Phys.: Condens. Matter.* **2009**, *21*, 375105.
[27] J. Lin, A. Kolomeisky, A. Meller, *Phys. Rev. Lett.* **2010**, *104*, 158101.
[28] W. Saenger, *Principles of Nucleic Acid Structure*, Springer-Verlag, New York, **1984**.
[29] W. Saenger, J. Riecke, D. Suck, *J. Mol. Biol.* **1975**, *93*, 529.
[30] Y. Seol, G. M. Skinner, K. Visscher, *Phys. Rev. Lett.* **2004**, *93*, 118102.
[31] Y. Seol, G. M. Skinner, K. Visscher, A. Buhot, A. Halperin, *Phys. Rev. Lett.* **2007**, *98*, 158103.
[32] A. J. Storm, J. H. Chen, H. W. Zandbergen, C. Dekker, *Phys. Rev. E.* **2005**, *71*, 051903.
[33] M. Gershow, J. A. Golovchenko, *Nat. Nanotechnol.* **2007**, *2*, 775.
[34] M. Van Den Hout, V. Krudde, X. J. Janssen, N. H. Dekker, *Biophys. J.* **2010**, *99*, 3840.
[35] M. Wanunu, J. Sutin, B. McNally, A. Chow, A. Meller, *Biophys. J.* **2008**, *95*, 4716.
[36] M. Van Den Hout, A. R. Hall, Wu M Y, Zandbergen H W., C. Dekker, N. H. Dekker, *Nanotechnology* **2010**, *21*, 115304.
[37] M.-Y. Wu, R. M. M. Smeets, M. Zandbergen, U. Ziese, D. Krapf, P. E. Batson, N. H. Dekker, C. Dekker, H. W. Zandbergen, *Nano Lett.* **2008**, *9*, 479.
[38] U. F. Keyser, D. Krapf, B. N. Koeleman, R. M. M. Smeets, N. H. Dekker, C. Dekker, *Nano Lett.* **2005**, *5*, 2253.

Received: February 6, 2011
Revised: March 14, 2011
Published online:

